# Electronic Supplementary Information (ESI)

## $[Au_{18}(dppm)_6Cl_4]^{4+}$: Phosphine-Protected Gold Nanocluster with Rich Charge States

**Shan-Shan Zhang,[a,⊥] Ravithree D. Senanayake,[b,⊥] Quan-Qin Zhao,[a] Hai-Feng Su,[c,*] Christine M. Aikens,[*,b] Xing-Po Wang,[*, a,] Chen-Ho Tung,[a] Di Sun[*, a, c] and Lan-Sun Zheng[c]**

[a]Key Laboratory of Colloid and Interface Chemistry, Ministry of Education, School of Chemistry and Chemical Engineering, and State Key Laboratory of Crystal Materials, Shandong University, Jinan, 250100, People's Republic of China.

[b]Department of Chemistry, Kansas State University, Manhattan, Kansas 66506, USA. Email: cmaikens@ksu.edu

[c]State Key Laboratory for Physical Chemistry of Solid Surfaces and Department of Chemistry, College of Chemistry and Chemical Engineering, Xiamen University, Xiamen, 361005, People's Republic of China. Email: hfsu@xmu.edu.cn

[⊥]These authors contributed equally to this work.

## Experimental details

The precursor [$Au_2(dppm)_2Cl_2$] was synthesized via a literature procedure.[1] All reagents employed were commercially available and used as received without further purification. IR spectra were recorded on a PerkinElmer Spectrum Two in the frequency range of 4000-400 $cm^{-1}$. The elemental analyses (C and H) were determined on a Vario EL III analyzer. Powder X-ray diffraction (PXRD) data were collected on a Philips X'Pert Pro MPD X-ray diffractometer with CuKα radiation equipped with an X'Celerator detector. The UV-Vis spectra were recorded on a UV/Vis spectrophotometer (Evolution 220, ISA-220 accessory, Thermo Scientific). Mass spectra were recorded on an Agilent 6224 (Agilent Technologies, USA) ESI-TOF-MS spectrometer. Sample solutions are infused by a syringe pump at 4 μL/min. Data were acquired using the following settings: ESI capillary voltage was set at 4000 V (+) ion mode and 3500 V (−) ion mode and fragmentor at 200 V. The liquid nebulizer was set to 15 psig and the nitrogen drying gas was set to a flow rate of 4 L/min. Drying gas temperature was maintained at 150 °C. The data analyses of mass spectra were performed based on the isotope distribution patterns using Agilent MassHunter Workstation Data acquisition software (Version B.05.00). The reported *m/z* values represent monoisotopic mass of the most abundant peak within the isotope pattern. Morphology of the samples and elemental composition analyses were measured using an SU-8010 field emission scanning electron microscope (FESEM; Hitachi Ltd., Tokyo, Japan) equipped with a Bruker XFlash 6|60 energy dispersive X-ray spectroscopy (EDX, Bruker, Germany) detector. Thermogravimetric analysis (TGA) was performed on PerkinElmer STA 8000.

## X-ray Crystallography

Single crystal of **SD/Au18** with appropriate dimensions was chosen under an optical microscope and quickly coated with high vacuum grease (Dow Corning Corporation) to prevent decomposition. Intensity data and cell parameters were recorded at 173 K on a Bruker Apex II single crystal diffractometer, employing a Mo $K_\alpha$ radiation ($\lambda$ = 0.71073 Å) and a CCD area detector. The raw frame data were processed using SAINT and SADABS to yield the reflection data file.[2] The structure was solved using the charge-flipping algorithm, as implemented in the program *SUPERFLIP*[3] and refined by full-matrix least-squares techniques against $F_o^2$ using the SHELXL program[4] through the OLEX2 interface.[5] Hydrogen atoms at carbon were placed in calculated positions and refined isotropically by using a riding model. Appropriate restraints or constraints were applied to the geometry and the atomic displacement parameters of the atoms in the cluster. All structures were examined using the Addsym subroutine of PLATON[6] to ensure that no additional symmetry could be applied to the models. Pertinent crystallographic data collection and refinement parameters are collated in Table S1. Selected bond lengths and angles are collated in Table S2.

## Synthesis of $[Au_{18}(dppm)_6Cl_4]\cdot C_6H_6\cdot 3Cl\cdot PF_6$ (SD/Au18)

To a 12 mL solution (THF/MeOH; v:v = 3:1) of $[Au_2(dppm)_2Cl_2]$ (0.02 mmol, 24.6 mg) was added $^nBuNPF_6$ (0.02 mmol, 7.7 mg). The solution was stirred (800 rpm) for 15 min at 0 $^oC$. Then 1 mL $NaBH_4$ (0.26 mmol) aqueous solution (10 mg/mL, cold water) was added slowly into above solution under vigorous stirring (1500 rpm). After 20 min, 25 μL triethylamine (0.18 mmol) was added in. The mixture reacted very fast and the color was immediately changed from colorless to black. The reaction continued for 12 h at 0 °C. The resulted solution was dried by rotary evaporation under reduced pressure. The black powder was collected then dissolved in dichloromethane and the dark-red solution was filtered through a syringe filter with a pore size of 450 nm and was diffused by benzene to obtain black crystals with a yield of 32 %. Anal. Calcd for $C_{162}H_{144}Au_{18}Cl_7F_6P_{13}$ (**SD/Au18**) calcd (found): C, 30.40 (30.95); H, 2.27 (2.42) %. IR: 3003 (w), 1572 (w), 1484 (w), 1440 (m), 1186 (m), 1097 (m), 995 (w), 834 (s), 783 (m), 733 (s), 688 (s), 557 (m), 513 (s) $cm^{-1}$.

**Table S1: Crystal Data Collection and Structure Refinement for SD/Au18.**

| | |
|---|---|
| Empirical formula | $C_{162}H_{144}Au_{18}Cl_7F_6P_{13}$ |
| Formula weight | 6400.92 |
| Temperature/K | 173(2) |
| Crystal system | triclinic |
| Space group | *P*-1 |
| a/Å | 15.442(4) |
| b/Å | 15.608(4) |
| c/Å | 18.615(4) |
| α /° | 70.259(2) |
| β /° | 82.278(2) |
| γ /° | 90.156(2) |
| Volume/Å$^3$ | 4179.0(17) |
| Z | 1 |
| ρ calcg/cm$^3$ | 2.543 |
| μ /mm$^{-1}$ | 16.017 |
| F(000) | 2906.0 |
| Radiation | MoKα (λ = 0.71073) |
| 2Θ range for data collection/° | 2.776 to 50 |
| Reflections collected | 49605 |
| Independent reflections | 14723 [$R_{int}$ = 0.1924, $R_{sigma}$ = 0.1353] |
| Data/parameters | 14723/928 |
| Goodness-of-fit on $F^2$ | 1.014 |
| Final R indexes [I>=2 σ (I)] | $R_1$ = 0.0761, $wR_2$ = 0.1999 |
| Final R indexes [all data] | $R_1$ = 0.1272, $wR_2$ = 0.2566 |
| Largest diff. peak/hole / e Å$^{-3}$ | 5.20/-3.30 |

**Table S2: Selected bond lengths (Å) and angles (º) for SD/Au18.**

| | | | |
|---|---|---|---|
| Au1—Au2 | 2.8217 (16) | Au4—Au9 | 2.7585 (15) |
| Au1—Au3 | 2.7982 (16) | Au4—P2 | 2.281 (7) |
| Au1—Au4 | 2.8850 (15) | Au5—Au6 | 2.7551 (15) |
| Au1—Au5 | 2.9859 (16) | Au5—Au9 | 2.7790 (15) |
| Au1—Au6 | 2.7668 (15) | Au5—P6 | 2.287 (7) |
| Au1—P1 | 2.287 (7) | Au6—Au6$^{i}$ | 2.723 (2) |
| Au2—Au3 | 2.7649 (16) | Au6—Au7$^{i}$ | 2.8600 (13) |
| Au2—Au5 | 2.8999 (16) | Au6—Au7 | 2.8414 (15) |
| Au2—Au6 | 2.7377 (13) | Au6—Au8 | 2.8849 (15) |
| Au2—Au7 | 2.8740 (15) | Au6—Au8$^{i}$ | 2.8662 (15) |
| Au2—P5 | 2.283 (7) | Au6—Au9 | 2.7651 (14) |
| Au3—Au6 | 2.7473 (14) | Au7—Au8$^{i}$ | 2.7246 (14) |
| Au3—Au7 | 2.9843 (15) | Au7—Au9$^{i}$ | 2.9621 (15) |
| Au3—Au8 | 2.8930 (14) | Au7—Cl2 | 2.373 (7) |
| Au3—Au9$^{i}$ | 2.9529 (15) | Au8—Au7$^{i}$ | 2.7246 (14) |
| Au3—P3 | 2.316 (7) | Au8—Au9$^{i}$ | 2.8933 (16) |
| Au4—Au5 | 2.8350 (15) | Au8—Cl1 | 2.344 (7) |
| Au4—Au6 | 2.7431 (16) | Au9—P4$^{i}$ | 2.304 (7) |
| Au4—Au7$^{i}$ | 2.8619 (15) | | |
| Symmetry code: (i) −*x*+1, −*y*+1, −*z*+1. | | | |

**Figure S1: The compared powder X-ray diffraction (PXRD) patterns of SD/Au18.**

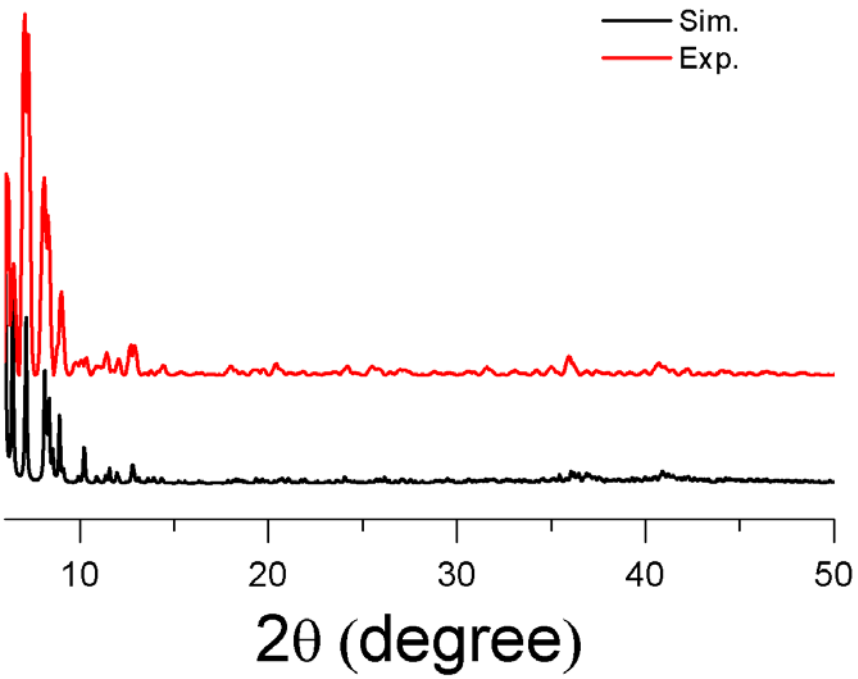

**Figure S2: The IR spectrum of SD/Au18.**

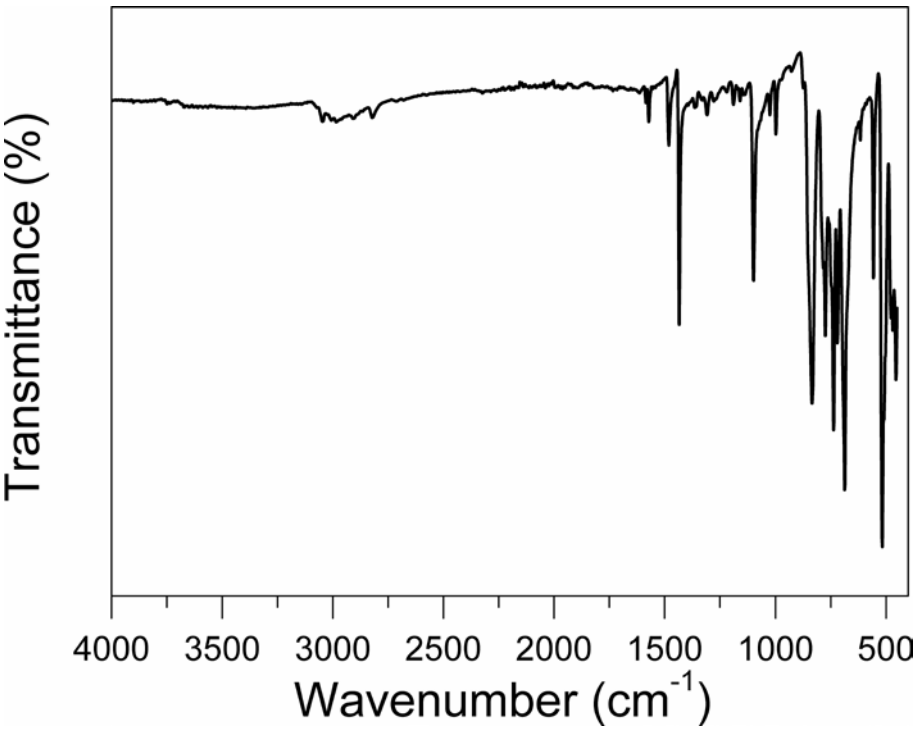

**Figure S3: Energy Dispersive X-Ray Spectroscopy (EDX) of SD/Au18.**

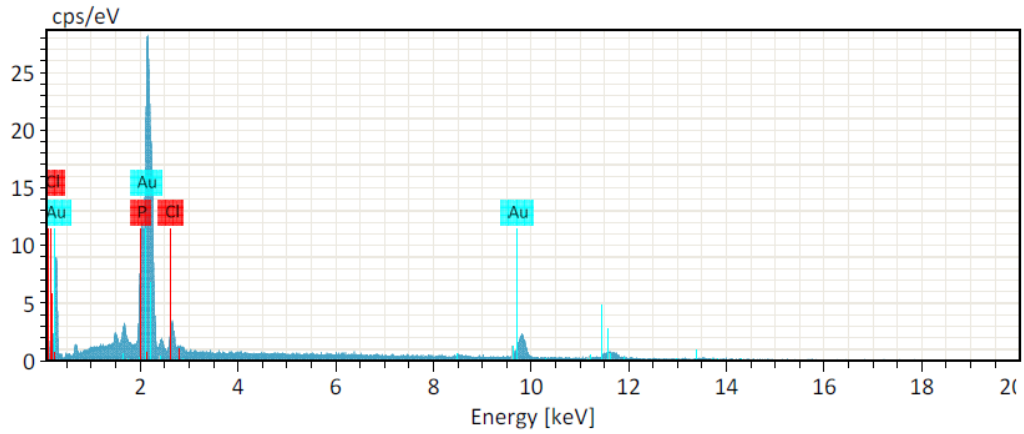

**Figure S4: TGA of SD/Au18.**

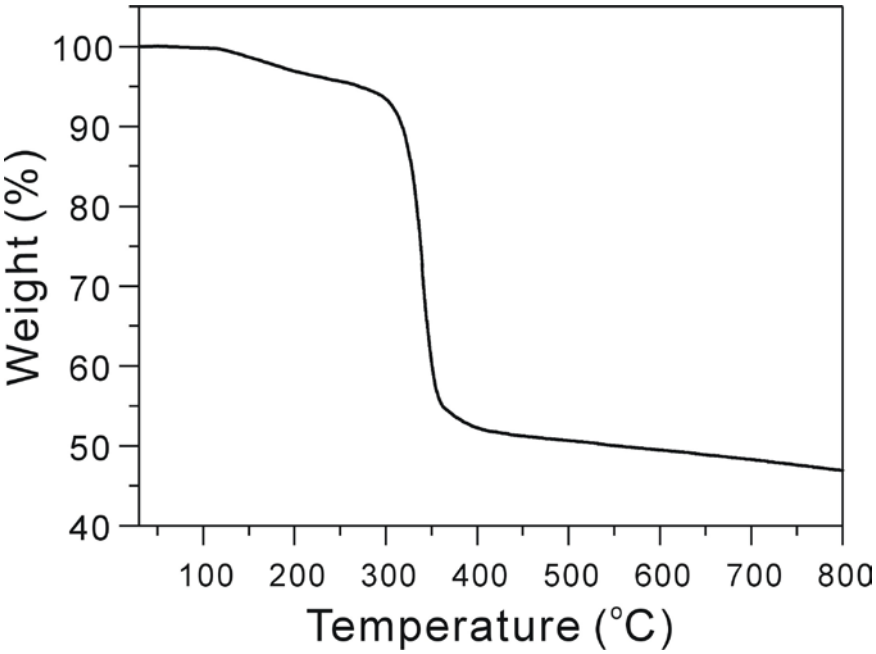

**Figure S5: Time-dependent UV-vis absorption spectra of SD/Au18.**

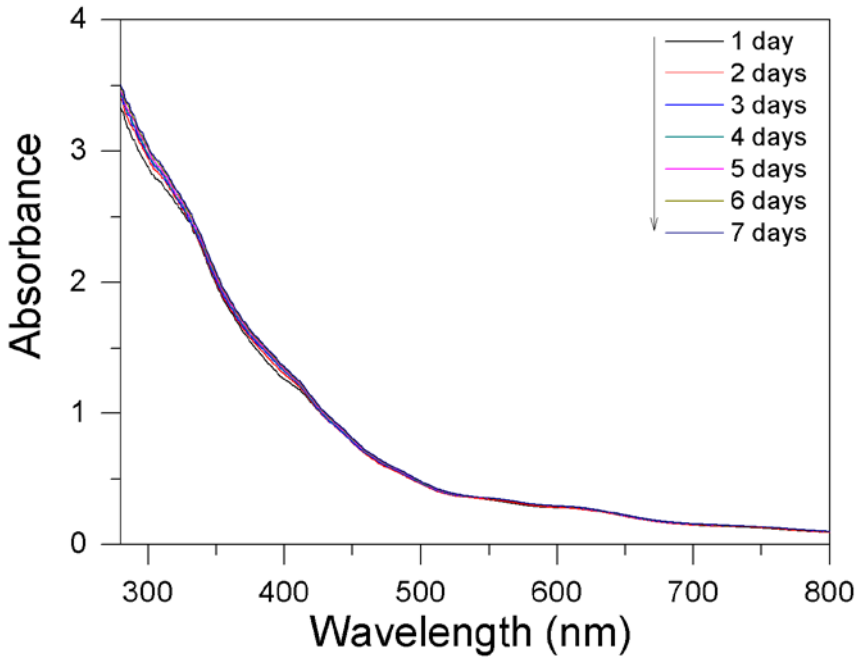

**Figure S6: The Morphology of the samples and elemental mapping of SD/Au18.**

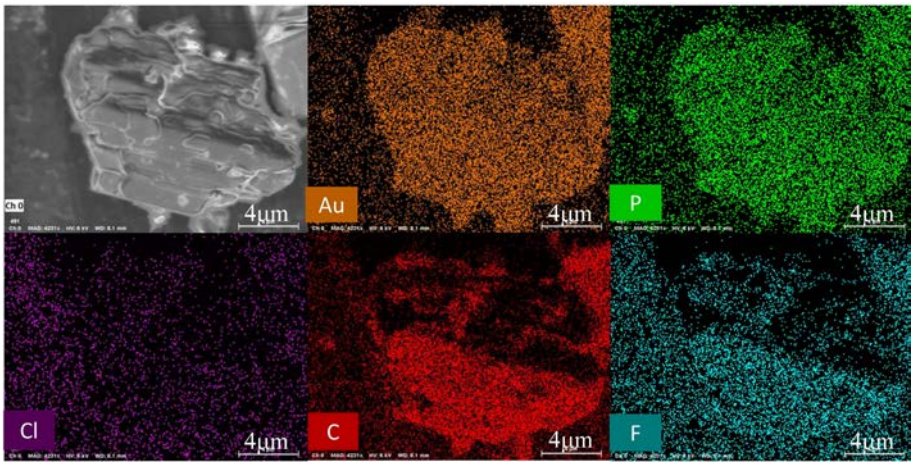

**Scheme S1: Photographs for crystals of SD/Au18 in mother liquor (left) and collected bulk sample of SD/Au18 (right) taken by the photographic camera under the ambient environment.**

## Computational Details

Density functional theory (DFT) calculations were performed on the $[Au_{18}(dppm)_6Cl_4]^{q+}$ and $[Au_{18}(PH_2CH_2PH_2)_6Cl_4]^{q+}$ systems ($q$ = 4, 2). The crystal structure of **SD/Au18** was used for the coordinates of $[Au_{18}(dppm)_6Cl_4]^{4+}$. In the model structure with $PH_2CH_2PH_2$ ligands, the P-H bond lengths were set to 1.435 Å. Time dependent DFT (TDDFT) calculations were performed on all systems to yield the absorption spectra using the LB94[7] model potential in the Amsterdam Density Functional (ADF)[8] package. ZORA[9] was used to treat the scalar relativistic effects for gold. Frozen core basis sets were employed for the crystal structure whereas full core basis set calculations were performed on the structure with $PH_2CH_2PH_2$ ligands. Plots of intensity vs. wavelength (nm) are fit with a Lorentzian with a full-width at half-maximum (FWHM) of 30 nm. The TDDFT calculations on the cluster were analyzed to get the most probable transitions and the orbitals responsible for each prominent peak in the calculated optical absorption spectra. The most probable transitions were identified based on the oscillator strength values, weights and the transition dipole moment values.

$[Au_{18}(dppm)_6Cl_4]^{2+}$ was found to have a HOMO-LUMO gap of 1.476 eV and $[Au_{18}(PH_2CH_2PH_2)_6Cl_4]^{2+}$ has a gap of 1.364 eV. $[Au_{18}(PH_2CH_2PH_2)_6Cl_4]^{4+}$ resulted in a very small HOMO-LUMO gap of 0.026 eV whereas the full ligand system $[Au_{18}(dppm)_6Cl_4]^{4+}$ did not converge (non-aufbau error). Reduced electron smearing (mixing 0.1, 0.05) values were tested on $[Au_{18}(PH_2CH_2PH_2)_6Cl_4]^{4+}$ but these did not change the small HOMO-LUMO gap. The effect of solvation by ethanol and chloroform was also considered by using the Conductor-like Screening Model (COSMO) implicit solvation model, which did not affect the small HOMO-LUMO gap of $[Au_{18}(PH_2CH_2PH_2)_6Cl_4]^{4+}$. Different numerical SCF convergence methods were tested on $[Au_{18}(dppm)_6Cl_4]^{4+}$ with the reduced smearing; however, the SCF did not converge. Triplet states were considered in addition to singlet states for the $[Au_{18}(dppm)_6Cl_4]^{4+}$ and $[Au_{18}(PH_2CH_2PH_2)_6Cl_4]^{4+}$ systems, but these calculations also did not converge.

**Table S3. Strong excitations in LB94/DZ spectrum of $[Au_{18}(PH_2CH_2PH_2)_6Cl_4]^{2+}$.**

| Excitation | Energy (eV) | Oscillator strength | Weight | Transition dipole moments | | | transitions |
|---|---|---|---|---|---|---|---|
| | | | | x | y | z | |
| 2 | 1.47 | 0.0310 | 0.9417 | 0.7074 | 0.3205 | -3.3272 | HOMO - LUMO |
| 5 | 1.81 | 0.0284 | 0.85 | -0.007 | 0.7823 | 2.8886 | HOMO-1 - LUMO+1 |
| 8 | 1.89 | 0.0101 | 0.4494 | 1.153 | 1.671 | -0.2849 | HOMO-2 - LUMO+1 |
| | | | 0.4067 | 1.198 | -0.1234 | 0.2243 | HOMO - LUMO+3 |
| | | | 0.0794 | -0.4126 | -0.8094 | -0.1399 | HOMO - LUMO+4 |
| 14 | 2.17 | 0.0166 | 0.6363 | -1.089 | -2.1361 | -0.3692 | HOMO - LUMO+4 |
| | | | 0.0812 | 0.0429 | 0.96 | 0.1046 | HOMO-3 - LUMO+3 |
| | | | 0.074 | -0.0135 | 0.3689 | 0.0908 | HOMO-5 - LUMO |
| 18 | 2.22 | 0.1477 | 0.6156 | 0.6724 | -0.2964 | -3.2399 | HOMO-2 - LUMO+2 |
| | | | 0.1515 | -0.5085 | 0.026 | 0.1486 | HOMO-6 - LUMO |
| | | | 0.0478 | 0.2176 | 0.4725 | -0.2796 | HOMO-1 - LUMO+2 |
| 21 | 2.27 | 0.0197 | 0.6938 | 0.0403 | -1.1049 | -0.272 | HOMO-5 - LUMO |
| | | | 0.1306 | -0.0258 | 0.6176 | -0.0036 | HOMO - LUMO+6 |
| 22 | 2.28 | 0.0372 | 0.5231 | -0.9314 | 0.0476 | 0.2721 | HOMO-6 - LUMO |
| | | | 0.1816 | 0.889 | -0.4864 | 0.2862 | HOMO-7 - LUMO |
| | | | 0.1459 | -0.0272 | 0.6508 | -0.0038 | HOMO - LUMO+6 |
| 26 | 2.35 | 0.0139 | 0.6141 | 1.6131 | -0.8826 | 0.5194 | HOMO-7 - LUMO |
| | | | 0.1815 | 0.5413 | -0.0277 | -0.1582 | HOMO-6 - LUMO |
| 29 | 2.42 | 0.0157 | 0.3439 | -0.2083 | -0.1802 | -0.016 | HOMO-8 - LUMO+1 |
| | | | 0.2929 | 0.0772 | 1.7265 | 0.1881 | HOMO-3 - LUMO+3 |
| | | | 0.1427 | -0.3082 | -0.5663 | -0.4954 | HOMO-1 - LUMO+5 |

**Table S4. Strong excitations in LB94/DZ spectrum of $[Au_{18}(dppm)_6Cl_4]^{2+}$.**

| Excitation | Energy (eV) | Oscillator strength | Weight | Transition dipole moments | | | transitions |
|---|---|---|---|---|---|---|---|
| | | | | x | y | z | |
| 2 | 1.54 | 0.0305 | 0.8365 | -0.7918 | -0.3835 | 3.0131 | HOMO - LUMO |
| 6 | 1.70 | 0.0183 | 0.4466 | 0.0739 | 0.7304 | 1.6722 | HOMO-1 - LUMO+1 |
| | | | 0.2063 | 0.2345 | 0.0534 | 0.5946 | HOMO - LUMO+2 |
| | | | 0.191 | 0.039 | -0.1345 | -0.171 | HOMO - LUMO+4 |
| 9 | 1.73 | 0.0499 | 0.6048 | -1.1775 | -1.3814 | 1.1995 | HOMO-2 - LUMO+1 |
| | | | 0.1823 | -0.0377 | 0.1302 | 0.1656 | HOMO - LUMO+4 |
| 20 | 1.94 | 0.0210 | 0.6624 | 0.8333 | 0.7878 | 0.7617 | HOMO-2 - LUMO+5 |
| 32 | 2.07 | 0.0572 | 0.4906 | -0.0348 | -0.0704 | -0.0357 | HOMO - LUMO+14 |
| | | | 0.334 | 0.5341 | -0.3838 | -1.6176 | HOMO-2 - LUMO+7 |
| 33 | 2.08 | 0.0492 | 0.481 | 0.0344 | 0.0696 | 0.0353 | HOMO - LUMO+14 |
| | | | 0.3262 | 0.5272 | -0.3789 | -1.5967 | HOMO-2 - LUMO+7 |
| 35 | 2.12 | 0.0224 | 0.8476 | -0.4532 | -0.3154 | -0.8091 | HOMO-1 - LUMO+8 |
| 42 | 2.16 | 0.0352 | 0.4506 | -0.2974 | -0.8553 | 0.5911 | HOMO-2 - LUMO+8 |
| | | | 0.3285 | -0.1849 | 0.4001 | 0.2367 | HOMO-3 - LUMO+2 |
| 46 | 2.20 | 0.0161 | 0.5221 | 0.4116 | 0.6071 | 0.0929 | HOMO - LUMO+19 |
| | | | 0.1999 | 0.4507 | 0.6896 | -0.0497 | HOMO-1 - LUMO+11 |
| 66 | 2.32 | 0.0110 | 0.7332 | -0.229 | 0.2129 | 0.5764 | HOMO-2 - LUMO+16 |
| | | | 0.1841 | -0.1739 | -0.2285 | -0.1429 | HOMO-2 - LUMO+17 |
| 80 | 2.42 | 0.0196 | 0.3498 | -0.2149 | -1.697 | -0.0674 | HOMO-3 - LUMO+6 |
| | | | 0.132 | 0.1112 | 0.3139 | 0.0061 | HOMO - LUMO+32 |
| | | | 0.1122 | 0.2154 | 0.1839 | 0.0436 | HOMO - LUMO+30 |
| | | | 0.1015 | 0.0771 | 0.2357 | -0.3868 | HOMO-1 - LUMO+21 |
| 88 | 2.47 | 0.0128 | 0.459 | 0.292 | -0.1306 | -1.0318 | HOMO-2 - LUMO+21 |
| | | | 0.214 | 0.0003 | 0.1418 | 0.3202 | HOMO-2 - LUMO+23 |
| 89 | 2.48 | 0.0182 | 0.2083 | 0.138 | 0.3894 | 0.0075 | HOMO - LUMO+32 |
| | | | 0.1703 | -0.2112 | -0.4509 | -0.1326 | HOMO-3 - LUMO+9 |
| | | | 0.1328 | 0.0967 | 0.2478 | -0.0734 | HOMO-1 - LUMO+23 |

## References


1. Ivan J. B. Lin, J. M. Hwang, D-F Feng, M. C. Cheng, Y. Wang, *Inorg. Chem.* 1994, **33**, 3467-3472.
2. *APEX3*, *SAINT* and *SADABS*. Bruker AXS Inc., Madison, Wisconsin, USA, 2015.
3. Palatinus, L.; Chapuis, G. *J. Appl. Crystallogr.* 2007, **40**, 786.
4. Sheldrick, G. M. *Acta. Crystallogr. Sect. C* 2015, **71**, 3.
5. Dolomanov, O. V.; Bourhis, L. J.; Gildea, R. J.; Howard, J. A. K.; Puschmann, H. *J. Appl. Crystallogr*. 2009, **42**, 339.
6. Spek, A. L. *Acta. Crystallogr. Sect*. D. 2009, **65**, 148.
7. Van Leeuwen, R.; Baerends, E. *Phys. Rev. A* 1994, **49**, 2421.
8. Te Velde, G.; Bickelhaupt, F. M.; Baerends, E. J.; Fonseca Guerra, C.; van Gisbergen, S. J.; Snijders, J. G.; Ziegler, T. *J. Comput. Chem.* 2001, **22**, 931.
9. van Lenthe, E.; Baerends, E.-J.; Snijders, J. G. *J. Chem. Phys.* 1993, **99**, 4597.